Original Article

LncRNA MAGI2-AS3 acts as a tumor suppressor that attenuates non-small cell lung cancer progression by targeting the miR-629-5p/TXNIP axis

Jun Gong[1#], Lei Ma[2#], Chunlei Peng[1], Jianhua Liu[3]

[1]Department of Medical Oncology, Affiliated Cancer Hospital of Nantong University, Nantong, China; [2]Department of Oncology, The Sixth People's Hospital of Nantong, Nantong, China; [3]Department of Oncology, Haimen People's Hospital, Nantong, China

Contributions: (I) Conception and design: J Gong; (II) Administrative support: L Ma; (III) Provision of study materials or patients: C Peng; (IV) Collection and assembly of data: J Liu; (V) Data analysis and interpretation: L Ma; (VI) Manuscript writing: All authors; (VII) Final approval of manuscript: All authors.

[#]These authors contributed equally to this work.

Correspondence to: Chunlei Peng. Department of Medical Oncology, Affiliated Cancer Hospital of Nantong University, Nantong 226001, China. Email: NTF126@126.com; Jianhua Liu. Department of Oncology, Haimen People's Hospital, Nantong 226100, China. Email: jshmliujh@163.com.

Background: Lung cancer is a malignant tumor that seriously threatens the health of human beings. Long non-coding RNAs (lncRNAs) are thought to play important roles in the pathophysiology of lung cancer. In this study, we identified a new lncRNA, MAGI2-AS3 in non-small cell lung cancer (NSCLC) tissues by conducting an integrated bioinformatics analysis. Mechanistic studies were also performed to explore the biological functions of MAGI2-AS3 in NSCLC progression.

Methods: A bioinformatics analysis was conducted to determine the prognostic role of MAGI2-AS3. CCK-8, EdU assay, colony formation and Transwell were performed to determine the effects of MAGI2-AS3 on the progression of NSCLC cells. A nude mice model was used to evaluate the effects of MAGI2-AS2 on the *in vivo* tumor growth of NSCLC. Luciferase reporter and RNA pull-down assays were used to evaluate interactions between MAGI2-AS3 and its downstream targets.

Results: MAGI2-AS3 was found to be downregulated in NSCLC tissues. The gain-of-function *in vitro* studies showed that the overexpression of MAGI2-AS3 suppressed NSCLC cell proliferation and invasion. Conversely, the knockdown of MAGI2-AS3 had the opposite effects. The bioinformatics analysis and luciferase report assay revealed that MAGI2-AS3 functioned as competing endogenous RNA to suppress microRNA (miR)-629-5p expression, while miR-629-5p suppressed thioredoxin-interacting protein (TXNIP) expression by targeting its 3' untranslated region. The rescue experiment results showed that MAGI2-AS3 knockdown enhanced NSCLC cell progression (increasing cell proliferation and invasion, but reducing cell apoptosis), which was counteracted by miR-629-5p inhibition or TXNIP overexpression.

Conclusions: The study revealed that MAGI2-AS3 was downregulated in NSCLC tissues and cells, and MAGI2-AS3 suppressed NSCLC cell progression. Further, the mechanistic results showed that MAGI2-AS3 exerted a tumor-suppressive effect in NSCLC by targeting the miR-629-5p/TXNIP axis.

Keywords: Non-small-cell lung cancer (NSCLC); MAGI2-AS3; miR-629-5p; thioredoxin-interacting protein (TXNIP); proliferation

Submitted Nov 02, 2021. Accepted for publication Dec 22, 2021.
doi: 10.21037/atm-21-6466
View this article at: https://dx.doi.org/10.21037/atm-21-6466

Introduction

Lung cancer is one of the most common human malignancies worldwide. Non-small-cell lung cancers (NSCLCs) account for more than 80% of all lung cancers (1). Based on pathological features, NSCLC can be classified into 3 subtypes: lung adenocarcinoma (LAD), large cell carcinoma (LCC), and lung squamous cell carcinoma (LSCC) (2,3). LSCC and LAD account for ~40% and ~50% of all NSCLC cases, respectively (2,3). Traditional therapeutic strategies have been greatly improved and targeted therapies, including as tyrosine kinase inhibitors of the epidermal growth factor receptor and immune checkpoint inhibitors, have been applied in NSCLC treatment; however, the 5-year overall survival rate of NSCLC remains less than 20% (4-6). The poor clinical outcomes of NSCLC patients could be attributed to the lack of early diagnostic biomarkers and therapeutic targets, and an insufficient understanding of the pathogenesis of NSCLC (7,8). To date, no precise molecular mechanism or relevant target have been identified in NSCLC progression or in the effective prediction of NSCLC metastasis. Thus, the molecular mechanism underlying NSCL progression needs to be urgently explored from a new perspective.

Research from the Human Genome Project shows that only about 19,000 genes (approximately 1–2% of the entire genome) encode proteins; the remaining 98–99% comprise "dark matter" non-coding sequences. Due to advances in next generation sequencing, the important role of long non-coding ribonucleic acid (lncRNA), which was originally regarded as transcription noise, has gradually been revealed. LncRNA is a non-coding RNA with a transcript length of more than 200 bases. It has a wide tissue expression profile and tissue expression specificity (9). There is increasing evidence that LncRNA can regulate gene function through multiple mechanisms, thereby affecting the biological function of tumor cells, and that it plays a role in promoting or inhibiting tumors (10,11). For example, lncRNA Highly upregulated in liver cancer (HULC) was identified during the screening of a hepatocellular carcinoma-specific gene library, and was demonstrated to be aberrantly expressed in many types of tumors (12). The recent studies revealed that lncRNA MAGI2-AS3 exerted inhibitory functions in different cancer types. For instance, MAGI2-AS3 inhibits bladder cancer progression through MAGI2/PTEN/EMT axis (13). MAGI2-AS3 also inhibits tumor progression and angiogenesis by regulating ACY1 via interacting with transcription factor HEY1 in clear cell renal cell carcinoma (14). Therefore, anti-MAGI2-AS3 compounds or agents might serve as novel therapeutic strategies for cancer treatment. In addition, miRNA serves as an oncogene and contributes to the progression of lung cancer (15). miR-629-5p promotes the invasion of lung adenocarcinoma via increasing both tumor cell invasion and endothelial cell permeability (16). Additionally, a large number of lncRNA or miRNA are used for the early diagnosis and molecular typing of NSCLC.

In this study, we identified a new lncRNA (i.e., MAGI2-AS3) in NSCLC tissues using an integrated bioinformatics analysis, Mechanistic studies were also performed to explore the biological functions of MAGI2-AS3 in NSCLC progression. Our findings strongly suggested that MAGI2-AS3 participates in NSCLC progression and is a promising therapeutic target.

We present the following article in accordance with the ARRIVE reporting checklist (available at https://dx.doi.org/10.21037/atm-21-6466).

Methods

Collection of microarray data and data processing

The microarray data were retrieved from the Gene Expression Omnibus (GEO) database. The collected data sets included GSE51852, GSE52248, and GSE81089. iGEAK software was used to analyze the expression data sets between the NSCLC group and non-tumor group (17). The overlapping differentially expressed genes (DEGs) in the data sets are illustrated in a Venn diagram. The study was conducted in accordance with the Declaration of Helsinki (as revised in 2013).

Analysis of MAGI-AS23 using Gene Expression Profiling Interactive Analysis (GEPIA) database and KM-plotter tool

The expression profile of the MAGI-AS23, which identified from the overlapping genes, were analyzed using the Gene Expression Profiling Interactive Analysis (GEPIA) database (18). The association between MAGI-AS3 expression and the overall survival of patients with lung cancer was evaluated using the Kaplan-Meier (K-M)-plotter tool (19). A P value <0.05 was considered statistically significant.

Cell lines and cell culture

All the cell lines, including Beas-2B, A549, and H1299,

came from the Cell Bank of the Chinese Academy of Sciences (Shanghai, China). All the cells were cultured in Dulbecco's Modified Eagle Medium (Gibco, Waltham, USA), supplemented with 10% fetal bovine serum (FBS; Gibco), and 1% penicillin/streptomycin (Sigma-Aldrich, St. Louis, USA). The cells were grown in culture dishes and maintained in cell incubators in a humidified atmosphere of at 37 ℃ with 5% carbon dioxide.

QRT-PCR

Total RNA was extracted from the tissue samples or cell lines using TRIzol reagent (Takara, Dalian, China) in accordance with the manufacturer's guidelines. RNA was reversed transcribed into complementary deoxyribonucleic acid (cDNA) using random primers and a Reverse Transcription Kit (Takara). RNA concentration and purity were determined using Nanodrop 1000 spectrophotometer (Thermo Fisher Scientific, Waltham, USA). To evaluate the expression of lncRNA or messenger (mRNA), quantitative reverse transcription-polymerase chain reaction (qRT-PCR) was performed using SYBR Green PCR Master Mix (Takara, Dalian, China) with ABI7900 Biosystems (Applied Biosystems, Foster City, USA) with a miRNA-specific 5' primer and the mRQ 3' primer supplied with (Genechem Company, Shanghai, China). Relative expression was normalized to glyceraldehyde-3-phosphate dehydrogenase (GAPDH) or U6, and was determined using the $2^{-\Delta\Delta Ct}$ method.

Cell transfection

To overexpress MAGI2-AS1 or thioredoxin-interacting protein (TXNIP), pcDNA3.1 vector (Genechem Company, Shanghai, China) were subcloned with MAGI2-AS3 or TXNIP (pcDNA-MAGI2-AS1, pcDNA-TXNIP). Empty pcDNA3.1 vector was used as the negative control. The short hairpin RNAs (shRNAs) against MAGI2-AS3 (sh-MAGI2-AS3#1/2: 5'-CCGGTTATAGGAAAGCTTTTA TCTTCTCGAGAAGATAAAAGCTTTCCTATAATTT TTG-3') were designed and synthesized by GenePharma (Shanghai, China). To overexpress miR-629-5p, miR-629-5p mimics were transfected into NSCLC cell lines. To silence miR-629-5p, miR-629-5p inhibitor was transfected into NSCLC cells. For the cell transfection, A549 and H1299 cell lines were planted in 6-well plates at around 80% confluence. Lipofectamine 2000 (Invitrogen, Carlsbad, CA, USA) was used for the transfection in accordance with the manufacturer's protocol. After 24 h, the cells were used for subsequent experiments.

Cell proliferation assays

For the cell counting kit 8 (CCK-8) assays, cells with different treatments were harvested and seeded in 96-well plates. Cell viability at different time points was assessed using the CCK-8 reagent (DOJINDO, Kumamoto, Japan) in accordance with the manufacturer's protocol. At 450 nm, absorbance was evaluated using a microplate reader.

For the colony formation assays, cells with different treatments were plated into 6-well plates at 500 cells per well. After culturing for 2 weeks, the cells were fixed in 4% paraformaldehyde for 10 min, and then stained with 0.1% crystal violet for 30 min. Finally, the colonies were counted and recorded under a light microscope.

For the EdU incorporation assays, A549 and H1299 cell lines on sterile coverslips were seeded in 24-well plates. Cell proliferation was detected using an EdU incorporation assay kit (Ribobio, Guangzhou, China). The nuclei were double-stained with EdU and 4′,6-diamidino-2-phenylindole (DAPI, Beyotime, Shanghai, China). The stained cells were visualized using a fluorescent microscope.

Transwell invasion assays

For the Transwell invasion assays, cells that underwent different treatments were added to the upper surface of matrigel-coated transwell chambers (BD Biosciences, San Jose, USA) with inserts containing 12-μm pore-size membrane. The lower chambers were filled with complete medium supplemented with 10% FBS. After culturing for 24 h, the invasive cells in the lower chambers were fixed with 4% paraformaldehyde, and then stained with 0.1% crystal violet. The invaded cells were counted using a light microscope.

Western blotting

Protein samples from tissues or cells were extracted using a radioimmunoprecipitation assay buffer supplemented with proteinase inhibitors (Beyotime, Beijing, China) and separated on 10% sodium dodecyl sulfate polyacrylamide gel electrophoresis by electrophoresis. After being transferred onto polyvinylidene fluoride membranes, the proteins were blocked with 5% skimmed milk at room temperature for 1 h. Subsequently, the polyvinylidene

fluoride membranes were incubated with primary antibodies against TXNIP (Abcam, Cambridge, UK) and β-actin (Abcam) at 4 ℃ overnight. Next, the membranes were incubated with corresponding secondary antibodies conjugated to horseradish peroxidase. The immunoreactive band were visualized using an enhanced chemiluminescence substrate kit (Pierce, Rockford, USA). β-actin was used as the internal reference.

RNA pull-down assays

The cells that underwent different treatments were transfected with a biotinylated-MAGI2-AS3 (wild type or mutants), and were trypsinized and homogenized. The RNA pull-down was performed on cell lysates using streptavidin-coated magnetic beads (Sigma-Aldrich). The bound mRNA was purified using the RNeasy mini kit (Qiagen, Hilden, Germany), and miR-629-5p expression in the bound fractions was examined by qPCR, and normalized to the "Input" controls.

Luciferase reporter assays

The amplified MAGI2-AS3 or 3' untranslated region (3'-UTR) of TXNIP was subcloned into the firefly plasmids in the pmirGLO luciferase vector (Promega, Madison, USA). The wild type of MAGI2-AS3 or TXNIP 3'-UTR was constructed. The site-directed mutation of miR-629-5p binding sites in MAGI2-AS1 or TXNIP 3'-UTR was generated using the Site-Directed Mutagenesis Kit (Invitrogen, Carlsbad, USA) in accordance with the manufacturer's protocol. The cells were separately co-transfected with different plasmids and miR-629-5p mimics or normal group (NC) mimics. 48 h after transfection, the Dual-Luciferase Reporter Assay System (Promega) was used to determine the relative luciferase activity.

Animal studies

Animal experiments were performed under a project license (No. 2021-0894) granted by the Animal Care and Use Committee, Affiliated Cancer Hospital of Nantong University, in compliance with the Guide for the Care and Use of Laboratory Animals of the Chinese Institutes of Health. To establish NSCLC-bearing xenograft models, 4-week-old male BALB/c nude mice were used in this study. Approximately 5×10^6 NSCLC cells with stably transfected pcDNA, pcDNA-MAGI2-AS3, lv-sh-MAGI2-AS3, or lv-sh-NC NSCLC cells were injected into the right flanks of the nude mice (there were 6 mice in each group). The length and width of tumors were measured with a digital caliper. Tumor volume was calculated using the following formula: volume = length × width × height ×0.5. Tumor size was measured every 5 days, and the mice were sacrificed 5 weeks after injection.

Statistical analysis

All the experimental data are presented as the mean ± standard deviation. GraphPad PRISM 6.0 (GraphPad, San Diego, USA) was used for the statistical analysis. Significant differences between and among treatment groups were evaluated using the Student's *t*-test or a 1-way analysis of variance followed by Bonferroni's post-hoc test. Differences were considered statistically significant if the P value was <0.05.

Results

MAGI2-AS3 was downregulated in NSCLC

First, we analyzed the 3 GEO data sets (i.e., GSE51852, GSE52248, and GSE81089), The DEGs in these data sets are visualized by volcano plots (*Figure 1A-1C*). In the GSE51852 data set, 3,471 DEGs (of which 1281 were upregulated and 2,190 were downregulated) were identified (*Figure 1A*). In the GSE52248 data set, 815 DEGs (of which 326 were upregulated and 489 were downregulated) were identified (*Figure 1B*). In the GSE81809 data set, 9,341 DEGs (of which 6,987 were upregulated and 2,354 were downregulated) were identified. Additionally, a total of 262 common DEGs were identified among the data sets (*Figure 1D*), one of which was lncRNA MAGI2-AS3. Based on the GEPIA analysis, the expression of MAGI2-AS3 was more downregulated in NSCLC tissues than normal lung tissues (*Figure 1E*). Similarly, the results of the KM-plotter analysis revealed that a high expression of MAGI2-AS3 was correlated with better overall survival in patients with lung cancer (*Figure 1F*).

MAGI2-AS3 suppressed NSCLC cell progression

To examine the role of MAGI2-AS3 in NSCLC progression, we performed *in vitro* functional studies. As expected, MAGI2-AS3 was more downregulated in the NSCLC cell lines than the normal NSCLC cells (*Figure 2A*). The

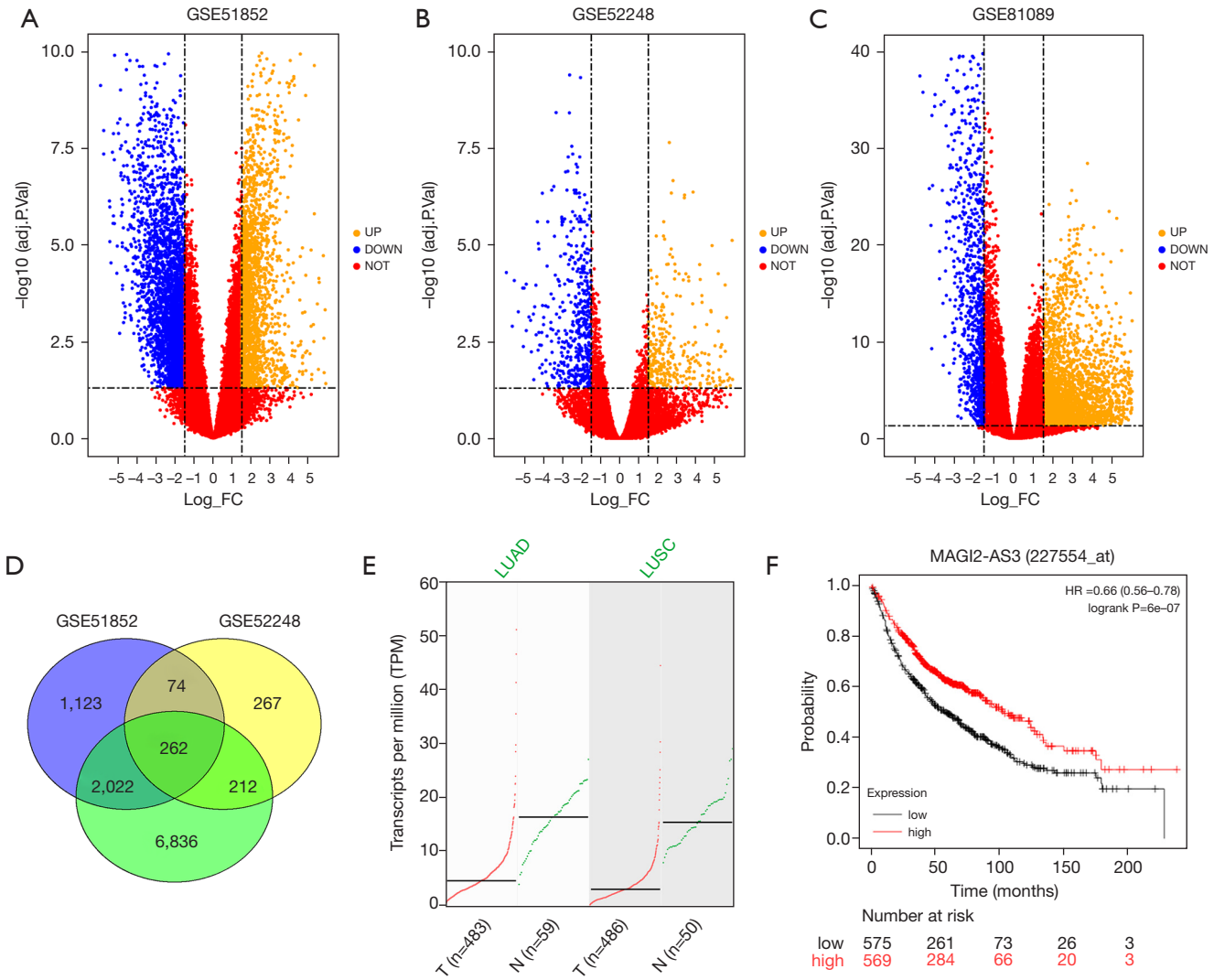

Figure 1 MAGI2-AS3 was downregulated in NSCLC. Volcano plots of differentially expressed genes in (A) GSE51852, (B) GSE52248, and (C) GSE81089. (D) Venn plot of the DEGs among GSE51852, GSE52248, and GSE81089; (E) expression of MAGI2-AS3 between non-tumor tissues and NSCLC tissues in the GEPIA data sets; (F) the association between MAGI2-AS3 expression and overall survival analysis of patients with lung cancer was evaluated using the KM-plotter tool. NSCLC, non-small cell lung cancer; DEGs, differentially expressed genes; GEPIA, Gene Expression Profiling Interactive Analysis.

overexpression of MAGI2-AS3 was achieved by transfecting A549 cells with pcDNA-MAGI2-AS3 vector (Figure S1A). The knockdown of MAGI2-AS3 was detected in H1299 cells transfected with MAGI2-AS3 shRNAs (Figure S1B). The overexpression of MAGI2-AS3 suppressed A549 cell proliferation and growth (*Figure 2B,2C*). Conversely, the knockdown of MAGI2-AS3 promoted H1299 cell proliferation and growth (*Figure 2D,2E*). Additionally, the overexpression of MAGI2-AS3 reduced the number of EdU-positive A549 cells (*Figure 2F*), while the knockdown of MAGI2-AS3 reduced the number of EdU-positive H1299 cells (*Figure 2G*). Further, MAGI2-AS3 overexpression impaired the invasive ability of A549 cells (*Figure 2H*), while H1299 cells with MAGI2-AS3 knockdown showed a decrease in casepase-3 activity (*Figure 2I*).

MAGI2-AS3 suppressed in vivo tumor growth

The effects of MAGI2-AS3 on *in vivo* tumor growth were evaluated in xenograft nude mice. As *Figure 3A,3B*

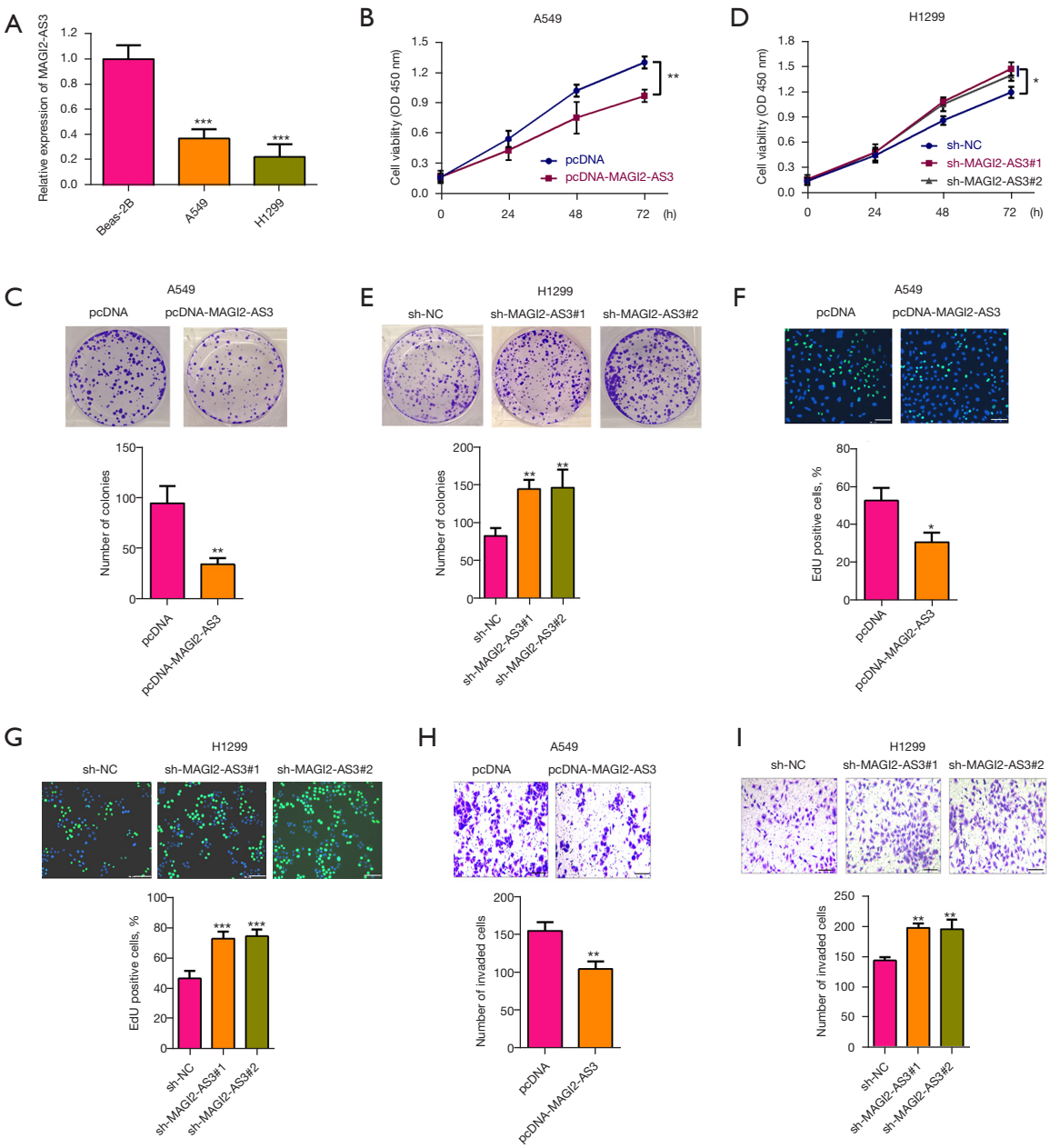

Figure 2 MAGI2-AS3 suppressed NSCLC cell progression. (A) MAGI2-AS3 expression in normal lung cells and NSCLC cell lines; (B) MAGI2-AS3 overexpression suppressed A549 cell proliferation; (C) MAGI2-AS3 overexpression suppressed A549 cell growth (crystal violet staining); (D) MAGI2-AS3 knockdown promoted H1299 cell proliferation; (E) MAGI2-AS3 knockdown promoted H1299 cell growth (crystal violet staining); (F) MAGI2-AS3 overexpression suppressed the EdU-positive cell number (double-stained with EdU; scale bar: 100 μm); (G) MAGI2-AS3 knockdown increased the EdU-positive cell number (double-stained with EdU; scale bar: 100 μm); (H) MAGI2-AS3 overexpression suppressed A549 invasion (crystal violet staining; scale bar: 100 μm); (I) MAGI2-AS3 knockdown increased the H1299 (crystal violet staining; scale bar: 100 μm). n=3, *P<0.05, **P<0.01, ***P<0.001. NSCLC, non-small cell lung cancer.

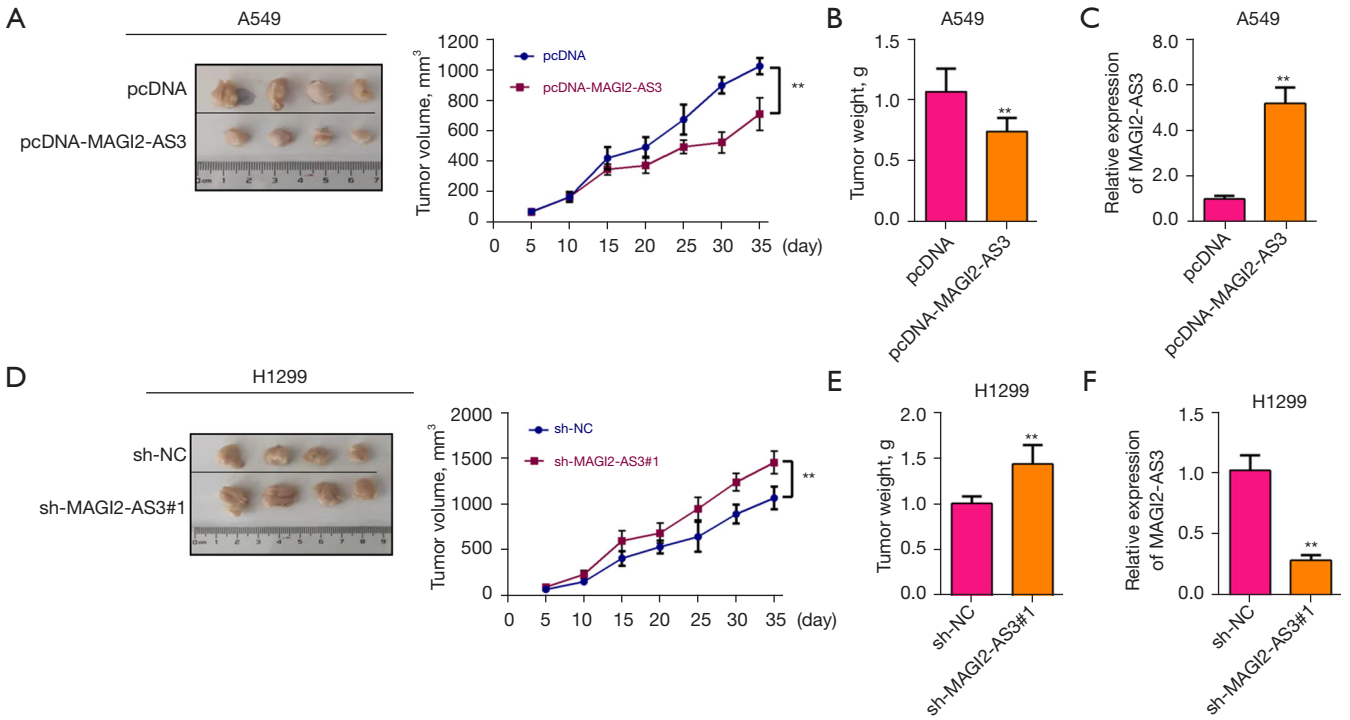

Figure 3 MAGI2-AS3 suppressed *in vivo* tumor growth. (A-C) MAGI2-AS3 overexpression suppressed *in vivo* tumor growth; (D-F) MAGI2-AS3 overexpression increase *in vivo* tumor growth. n=6, **P<0.01.

show, the overexpression of MAGI2-AS3 suppressed the *in vivo* tumor growth of A549 cells in the nude mice. Further, the expression of MAGI22-AS3 in tumor tissues was more upregulated in the pcDNA-MAGI22-AS3 group than the pcDNA group (*Figure 3C*). Conversely, the knockdown of MAGI2-AS3 enhanced the *in vivo* tumor growth of H1299 cells (*Figure 3D,3E*), and the expression of MAGI22-AS3 in the tumor tissues was more downregulated in the sh_MAGI22-AS3#1 group than the sh-NC group (*Figure 3E,3F*).

MAGI2-AS3 targets miR-629-5p and represses its expression

The downstream targets of MAGI2-AS3 were predicted by the Starbase online database. *Figure 4A* shows the binding sites between MAGI2-AS3 and miR-629-5p. The RNA pull-down results revealed that MAGI2-AS3 could bind to the miR-629-5p in A549 and H1299 cells (*Figure 4B*), and the mutation of the MAGI2-AS3 sequence could abolish the binding between MAGI2-AS3 and miR-629-5p (*Figure 4C*). The overexpression of MAGI2-AS3 suppressed miR-629-5p expression (*Figure 4D*), while the knockdown of MAGI2-AS3 increased miR-629-5p expression in H1299 cells (*Figure 4E*). The physical interaction was then confirmed by luciferase reporter assays. The overexpression of miR-629-5p was achieved by transfecting H1299 cells with miR-629-5p mimics (Figure S1C). The overexpression of miR-629-5p suppressed the luciferase activity of the wild-type MAGI2-AS3 cells, but not the mutant cells (*Figure 4F*).

MiR-629-5p targets TNXIP and represses its expression

The downstream targets of miR-629-5p were further predicted by the Starbase online database. *Figure 5A* shows that binding sites between miR-629-5p and TXNIP 3'-UTR. Overexpression of miR-629-5p down-regulated the expression of TXNIP in H1299 cells, while the transfection of miR-629-5p inhibitors suppressed the expression of miR-629-5p in H1299 cells (Figure S1D) and upregulated the expression of TXNIP in H1299 cells (*Figure 5B-5D*). Similarly, the knockdown of MAGI2-AS2 downregulated the expression of TXNIP in H1299 cells, while the overexpression of MAGI2-AS2 upregulated the expression of TXNIP in H1299 cells (*Figure 5E-5G*). The luciferase reporter assay showed that the overexpression

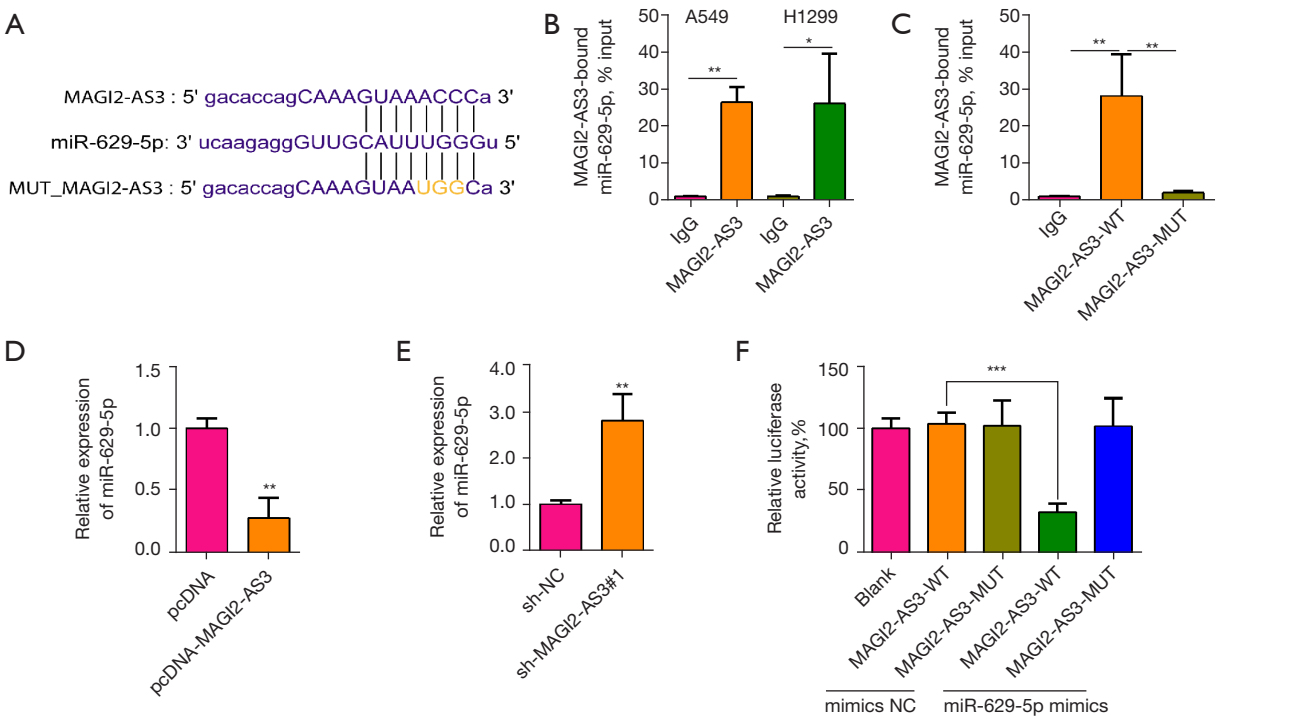

Figure 4 MAGI2-AS3 targets miR-629-5p and represses its expression. (A) Predicted binding targets between miR-629-5p and MAGI22-AS2; (B,C) RNA pull-down between miR-629-5p and MAGI2-AS3; (D,E) effects of MAGI22-AS3 on miR-629-5p expression; (F) luciferase activity of MAGI2-AS3-WT or -MUT in H1299 cells after the transfection of miR-629-5p mimics or NC mimics. n=3, *P<0.05, **P<0.01, ***P<0.001. WT, wild type; MUT, mutant type.

of miR-629-5p suppressed the luciferase activity of the wild-type TXNIP 3'-UTR cells, but not the mutant cells (*Figure 5H*). Further, *in vitro* rescue functional studies were performed to examine the interaction between miR-629-5p and TXNIP. The overexpression of miR-629-5p increased H1299 cell proliferation and invasion, while the oncogenic effects of miR-629-5p overexpression on H1299 cells were partially counteracted by the enforced expression of TXNIP (*Figure 5I-5L*).

MAGI2-AS3 modulates NSCLC progression by targeting the miR-629-5p/TXNIP axis

The interaction between MAGI2-AS3 and miR-629-5/TXNIP axis was further confirmed by rescue *in vitro* functional assays. As *Figure 6A,6B* show, the inhibition of miR-629-5p or the enforced expression of TXNIP attenuated the suppressive effects of MAGI2-AS3 knockdown on the expression of TXNIP in H1299 cells. The *in vitro* functional studies revealed that the knockdown of MAGI2-AS3 increased H1299 cell proliferation and invasion, and the oncogenic effects of MAGI2-AS3 knockdown on H1299 cells were partially counteracted by the inhibition of miR-629-5p or the enforced expression of TXNIP (*Figure 6C-6F*).

Discussion

Patients diagnosed with advanced/metastatic NSCLC often have a poor prognosis. Unfortunately, due to the unclear pathophysiology of this deadly malignancy, the therapies for advanced/metastatic NSCLC are limited. Recent studies from different research groups have emphasized the importance of lncRNAs in the pathophysiology of NSCLC. A growing number of lncRNAs have been shown to exert either oncogenic functions or tumor-suppressive functions in NSCLC (13). In the present study, we identified a new lncRNA (i.e., MAGI2-AS3) in NSCLC tissues using an integrated bioinformatics analysis, and this lncRNA was downregulated in the NSCLC tissues. The gain-of-function *in vitro* studies showed that the overexpression of MAGI2-AS3 suppressed NSCLC cell proliferation

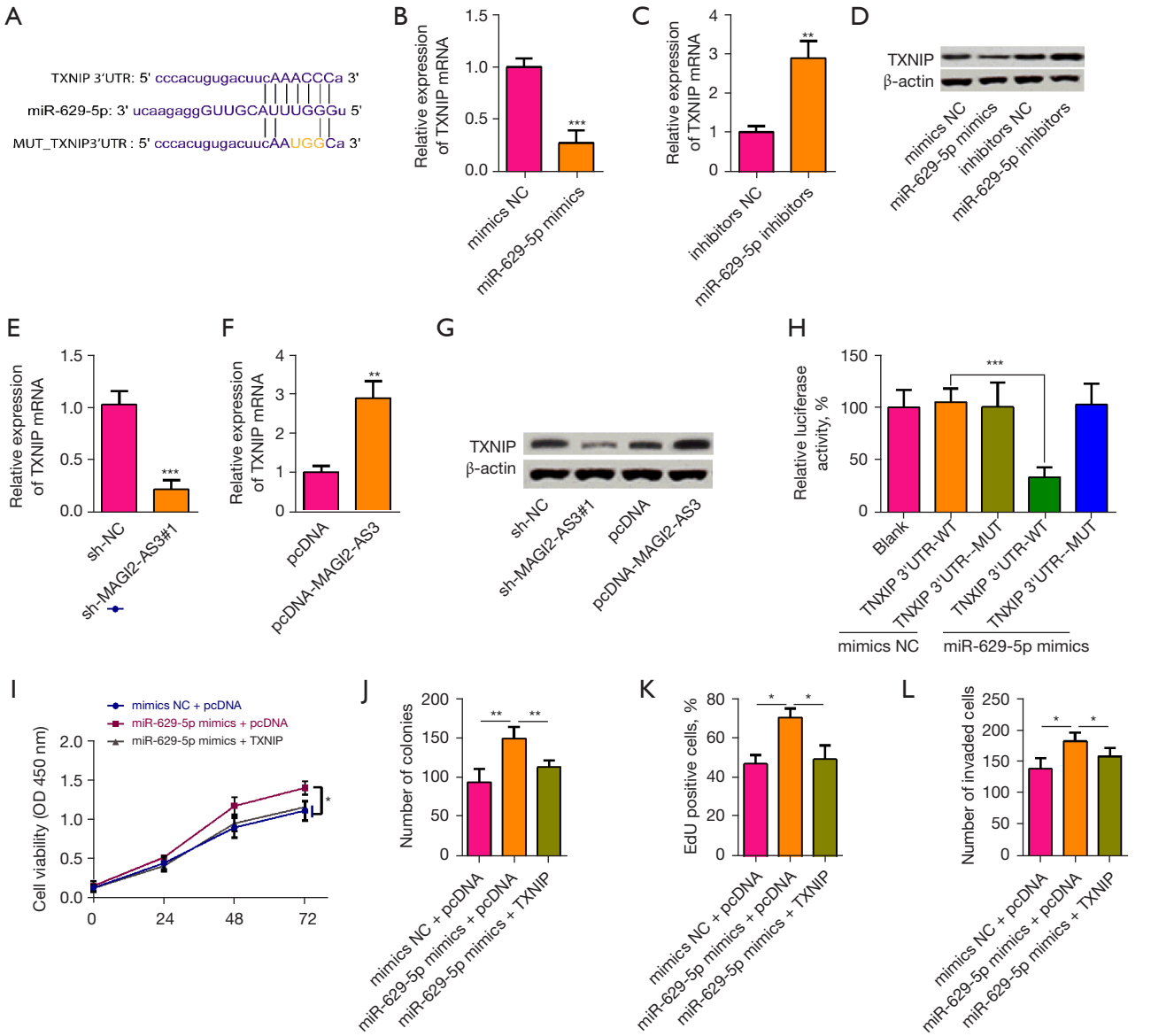

Figure 5 MiR-629-5p targets TNXIP and represses its expression. (A) Predicted bindings sites between miR-629-5p and TXNIP 3'-UTR; (B-F) effects of miR-629-6p and MAGI22-AS3 on TXNIP expression; (H) luciferase activity of TNXIP 3'-UTR-WT or -MUT in H1299 cells after the transfection of miR-629-5p mimics or NC mimics; (I-L) the overexpression of TXNIP counteracted the tumor-suppressive effects of miR-629-5p in H1299 cells. n=3, *P<0.05, **P<0.01, ***P<0.001. WT, wild type; MUT, mutant type.

and invasion, while the knockdown of MAGI2-AS3 had the opposite effects. The bioinformatics analysis in combination with the luciferase report assays revealed that MAGI2-AS3 functioned as a competing endogenous RNA to suppress miR-629-5p expression, while miR-629-5p suppressed TXNIP expression by targeting its 3'-UTR cells. The rescue experiment results showed that MAGI2-AS3 knockdown enhanced NSCLC cell progression (i.e., increased cell proliferation and invasion, but reduced cell apoptosis), which was counteracted by miR-629-5p inhibition or TXNIP overexpression. All the results suggest that the MAGI-AS3/miR-629-5p/TXNIP axis plays a key regulatory role in NSCLC progression.

LncRNAs are now regarded as important regulators in the progression of malignant tumors. The role of MAGI2-AS3 was first characterized by Yang *et al.*, who located

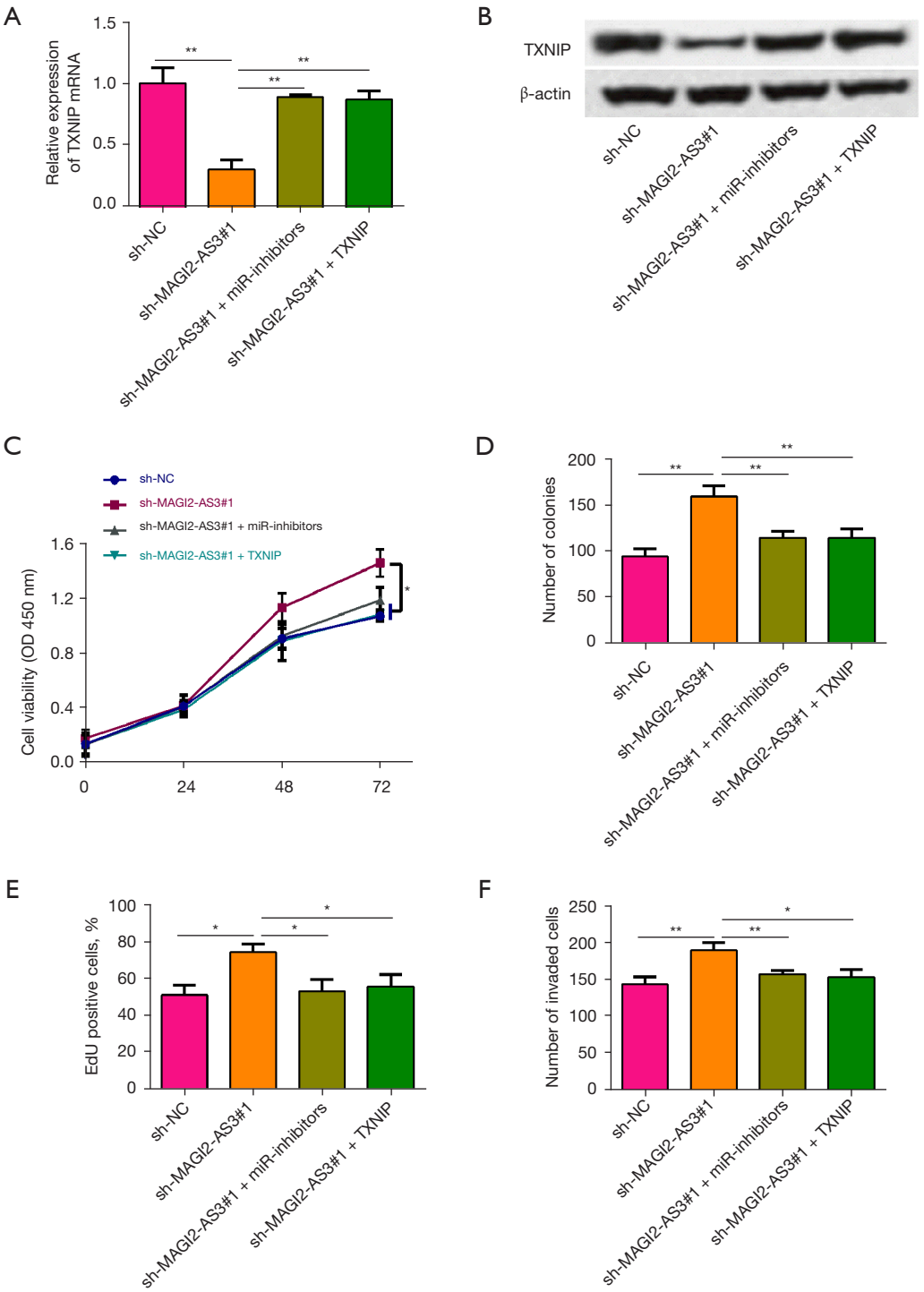

Figure 6 MAGI2-AS3 modulates NSCLC progression by targeting miR-629-5p/TXNIP axis. (A,B) Expression of TNXIP in NSCLC cells after different treatments; (C-F) the knockdown of miR-629-5p or overexpression of TXNIP countered the tumor-enhancing effects of MAGI22-AS3 knockdown on NSCLC. n=3, *P<0.05, **P<0.01. NSCLC, non-small cell lung cancer.

it on chromosome 7 (20). A later study by Wang *et al.*, showed that MAGI2-AS3 regulates CCDC19 expression by sponging miR-15b-5p, and suppresses bladder cancer progression (21). Pu *et al.* also found that lncRNA MAGI2-AS3 prevents the development of hepatocellular carcinoma by recruiting lysine-specific histone demethylase 1A (KDM1A) and promoting the H3K4me2 demethylation of the RACGAP1 promoter (22). Conversely, our results consistently showed that silencing MAGI2-AS3 suppressed NSCLC cell progression (decreasing cell proliferation and invasion, while increasing cell apoptosis). Further, the clinical sample evidence showing the downregulation of MAGI2-AS3 in NSCLC tissues implies that MAGI2-AS3 acts as a tumor suppressor in NSCLC.

LncRNAs commonly act as competing endogenous RNAs (ceRNAs) for miRNAs, and thus attenuate the suppressive effects of these miRNAs on target genes (23-25).

Privous studies have showed that MAGI2-AS3 inhibits bladder cancer progression through MAGI2/PTEN/EMT axis (13). In addition, MAGI2-AS3 also inhibits tumor progression and angiogenesis by regulating ACY1 via interacting with transcription factor HEY1 in clear cell renal cell carcinoma (14). Our bioinformatics analysis showed that MAGI2-AS3 could target various miRNAs, and that among these miRNAs, MAGI2-AS3 can bind to miR-629-5p, which has been proven to act as an oncogene in different types of cancers (16,26,27). Thus, we further studied miR-629-5p using luciferase reporter assays, and the results confirmed an interaction between miR-629-5p and MAGI2-AS3 in NSCLC cells. In the rescue experiments, miR-629-5p knockdown attenuated the tumor-enhancing effects of MAGI2-AS3 knockdown in NSCLC cells, which suggests that MAGI2-AS3 exerts a tumor-suppressive action by targeting miR-629-5p in NSCLC cells. Additionally, we also explored the downstream signaling of miR-629-5p, and TXNIP was identified as a target of miR-629-6p. TXNIP has been found to act as a tumor suppressor in NSCLC and other types of cancer (28-31). Our rescue experiments consistently showed that the overexpression of TXNIP attenuated the oncogenic actions of MAGI2-AS3 in NSCLC cells. Together, our results imply that MAGI2-AS3 regulates NSCLC cell progression by targeting the miR-629-5p/TXNIP axis.

Conclusions

In conclusion, the current investigation revealed that MAGI2-AS3 was downregulated in NSCLC tissues and NSCLC cells, and MAGI2-AS3 suppressed NSCLC cell progression. Further, our mechanistic results showed that MAGI2-AS3 exerted a tumor-suppressive function in NSCLC by targeting the miR-629-5p/TXNIP axis.

Acknowledgments

Funding: None.

Footnote

Reporting Checklist: The authors have completed the ARRIVE reporting checklist. Available at https://dx.doi.org/10.21037/atm-21-6466

Data Sharing Statement: Available at https://dx.doi.org/10.21037/atm-21-6466

Conflicts of Interest: All authors have completed the ICMJE uniform disclosure form (available at https://dx.doi.org/10.21037/atm-21-6466). The authors have no conflicts of interest to declare.

Ethical Statement: The authors are accountable for all aspects of the work in ensuring that questions related to the accuracy or integrity of any part of the work are appropriately investigated and resolved. The study was conducted in accordance with the Declaration of Helsinki (as revised in 2013). Animal experiments were performed under a project license (No. 2021-0894) granted by the Animal Care and Use Committee, Affiliated Cancer Hospital of Nantong University, in compliance with the Guide for the Care and Use of Laboratory Animals of the Chinese Institutes of Health.

References

1. Hirsch FR, Scagliotti GV, Mulshine JL, et al. Lung cancer:

current therapies and new targeted treatments. Lancet 2017;389:299-311.
2. Oser MG, Niederst MJ, Sequist LV, et al. Transformation from non-small-cell lung cancer to small-cell lung cancer: molecular drivers and cells of origin. Lancet Oncol 2015;16:e165-72.
3. van Meerbeeck JP, Fennell DA, De Ruysscher DK. Small-cell lung cancer. Lancet 2011;378:1741-55.
4. da Cunha Santos G, Shepherd FA, Tsao MS. EGFR mutations and lung cancer. Annu Rev Pathol 2011;6:49-69.
5. Russo A, Cardona AF, Caglevic C, et al. Overcoming TKI resistance in fusion-driven NSCLC: new generation inhibitors and rationale for combination strategies. Transl Lung Cancer Res 2020;9:2581-98.
6. Jonna S, Subramaniam DS. Molecular diagnostics and targeted therapies in non-small cell lung cancer (NSCLC): an update. Discov Med 2019;27:167-70.
7. Goldstraw P, Ball D, Jett JR, et al. Non-small-cell lung cancer. Lancet 2011;378:1727-40.
8. Tan WL, Jain A, Takano A, et al. Novel therapeutic targets on the horizon for lung cancer. Lancet Oncol 2016;17:e347-62.
9. Jathar S, Kumar V, Srivastava J, et al. Technological Developments in lncRNA Biology. Adv Exp Med Biol 2017;1008:283-323.
10. Peng WX, Koirala P, Mo YY. LncRNA-mediated regulation of cell signaling in cancer. Oncogene 2017;36:5661-7.
11. Ni C, Teng P, Hu P. Effects of ANCR lncRNA on the biological behaviors of lung cancer cells A549 and the mechanism. Transl Cancer Res 2020;9:4693-702.
12. Ghafouri-Fard S, Esmaeili M, Taheri M, et al. Highly upregulated in liver cancer (HULC): An update on its role in carcinogenesis. J Cell Physiol 2020;235:9071-9.
13. Shen D, Xu J, Cao X, et al. Long noncoding RNA MAGI2-AS3 inhibits bladder cancer progression through MAGI2/PTEN/epithelial-mesenchymal transition (EMT) axis. Cancer Biomark 2021;30:155-65.
14. Wang G, Li H, Hou Y. LncRNA MAGI2-AS3 inhibits tumor progression and angiogenesis by regulating ACY1 via interacting with transcription factor HEY1 in clear cell renal cell carcinoma. Cancer Gene Ther 2021. doi: 10.1038/s41417-021-00339-z. [Epub ahead of print].
15. Du X, Zhang J, Wang J, et al. Role of miRNA in Lung Cancer-Potential Biomarkers and Therapies. Curr Pharm Des 2018;23:5997-6010.
16. Li Y, Zhang H, Fan L, et al. MiR-629-5p promotes the invasion of lung adenocarcinoma via increasing both tumor cell invasion and endothelial cell permeability. Oncogene 2020;39:3473-88.
17. Choi K, Ratner N. iGEAK: an interactive gene expression analysis kit for seamless workflow using the R/shiny platform. BMC Genomics 2019;20:177.
18. Tang Z, Li C, Kang B, et al. GEPIA: a web server for cancer and normal gene expression profiling and interactive analyses. Nucleic Acids Res 2017;45:W98-W102.
19. Győrffy B, Surowiak P, Budczies J, et al. Online survival analysis software to assess the prognostic value of biomarkers using transcriptomic data in non-small-cell lung cancer. PLoS One 2013;8:e82241.
20. Yang Y, Yang H, Xu M, et al. Long non-coding RNA (lncRNA) MAGI2-AS3 inhibits breast cancer cell growth by targeting the Fas/FasL signalling pathway. Hum Cell 2018;31:232-41.
21. Wang F, Zu Y, Zhu S, et al. Long noncoding RNA MAGI2-AS3 regulates CCDC19 expression by sponging miR-15b-5p and suppresses bladder cancer progression. Biochem Biophys Res Commun 2018;507:231-5.
22. Pu J, Wang J, Wei H, et al. lncRNA MAGI2-AS3 Prevents the Development of HCC via Recruiting KDM1A and Promoting H3K4me2 Demethylation of the RACGAP1 Promoter. Mol Ther Nucleic Acids 2019;18:351-62.
23. He J, Zhou X, Li L, et al. Long Noncoding MAGI2-AS3 Suppresses Several Cellular Processes of Lung Squamous Cell Carcinoma Cells by Regulating miR-374a/b-5p/CADM2 Axis. Cancer Manag Res 2020;12:289-302.
24. Li F, Hu Q, Pang Z, et al. LncRNA MAGI2-AS3 Upregulates Cytokine Signaling 1 by Sponging miR-155 in Non-Small Cell Lung Cancer. Cancer Biother Radiopharm 2020;35:72-6.
25. Sui Y, Chi W, Feng L, et al. LncRNA MAGI2-AS3 is downregulated in non-small cell lung cancer and may be a sponge of miR-25. BMC Pulm Med 2020;20:59.
26. Lu J, Lu S, Li J, et al. MiR-629-5p promotes colorectal cancer progression through targetting CXXC finger protein 4. Biosci Rep 2018;38:BSR20180613.
27. Tao X, Yang X, Wu K, et al. miR-629-5p promotes growth and metastasis of hepatocellular carcinoma by activating beta-catenin. Exp Cell Res 2019;380:124-30.
28. Iqbal MA, Chattopadhyay S, Siddiqui FA, et al. Silibinin induces metabolic crisis in triple negative breast cancer cells by modulating EGFR-MYC-TXNIP axis: potential therapeutic implications. FEBS J 2021;288:471-85.
29. Li YH, Tong KL, Lu JL, et al. PRMT5-TRIM21 interaction regulates the senescence of osteosarcoma cells

by targeting the TXNIP/p21 axis. Aging (Albany NY) 2020;12:2507-29.
30. Yang SS, Ma S, Dou H, et al. Breast cancer-derived exosomes regulate cell invasion and metastasis in breast cancer via miR-146a to activate cancer associated fibroblasts in tumor microenvironment. Exp Cell Res 2020;391:111983.
31. Zhang J, Tian X, Yin H, et al. TXNIP induced by MondoA, rather than ChREBP, suppresses cervical cancer cell proliferation, migration and invasion. J Biochem 2020;167:371-7.

(English Language Editor: L. Huleatt)

Cite this article as: Gong J, Ma L, Peng C, Liu J. LncRNA MAGI2-AS3 acts as a tumor suppressor that attenuates non-small cell lung cancer progression by targeting the miR-629-5p/TXNIP axis. Ann Transl Med 2021;9(24):1793. doi: 10.21037/atm-21-6466

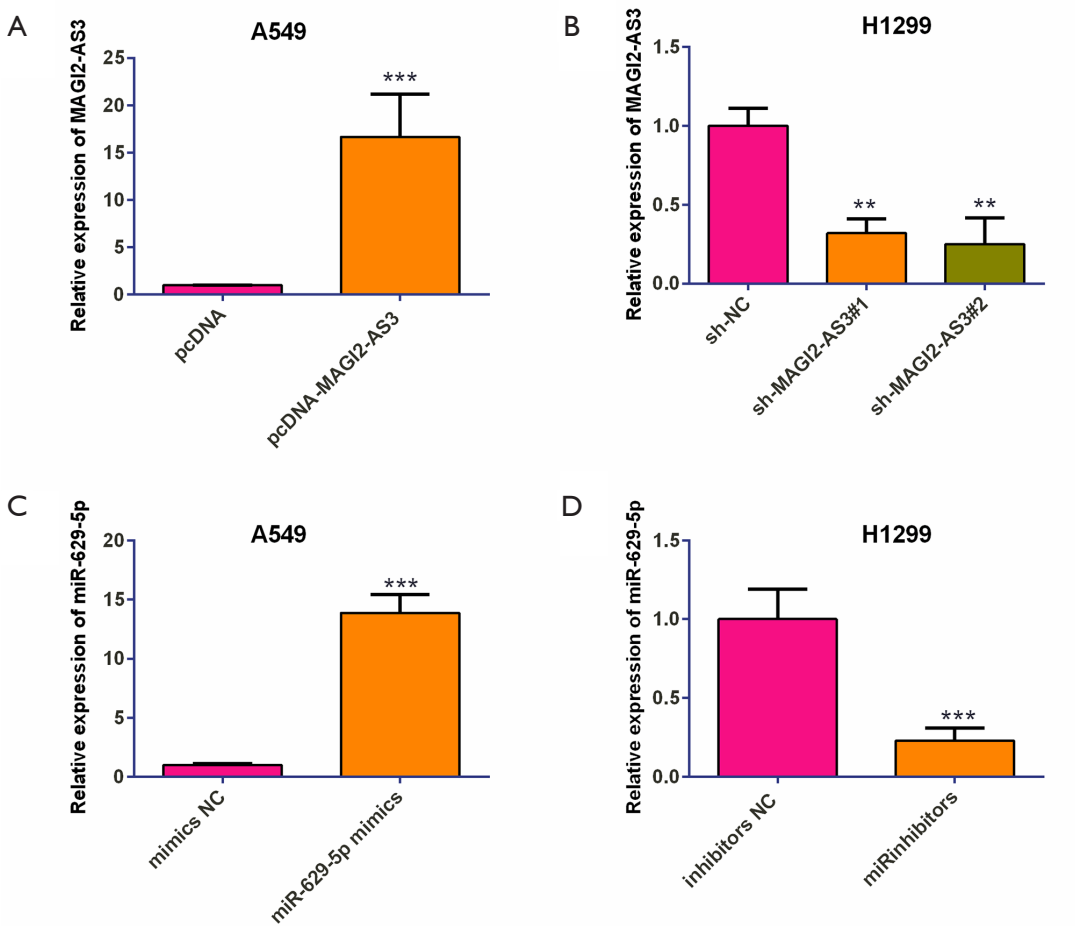

Figure S1 Expression of MAGI2-AS3 in A549 cells after (A) pcDNA or pcDNA-MAGI2-AS3 transfection; (B) sh-NC, sh-MAGI2-AS3#1, or sh-MAGI2-AS3#2 transfection. Expression of miR-629-5p in H1299 cells after the transfection (C) of mimics NC or miR-629-5p mimics; (D) inhibitors NC or miR-inhibitors. **P<0.01, ***P<0.001. NC, normal group.